RESEARCH ARTICLE | DECEMBER 08 2025

Ego-centered network intervention via weak-tie exclusion

Peng Chen ; Mingze Qi ; Zhi Zeng ; Xiaojun Duan ; Xin Lu

Chaos 35, 121103 (2025)
https://doi.org/10.1063/5.0307081

Ego-centered network intervention via weak-tie exclusion

Cite as: Chaos 35, 121103 (2025); doi: 10.1063/5.0307081
Submitted: 14 October 2025 · Accepted: 20 November 2025 ·
Published Online: 8 December 2025

Peng Chen,[1] Mingze Qi,[1,a)] Zhi Zeng,[1] Xiaojun Duan,[1,a)] and Xin Lu[2]

AFFILIATIONS

[1]College of Science, National University of Defense Technology, Changsha, Hunan 410073, People's Republic of China
[2]College of Systems Engineering, National University of Defense Technology, Changsha, Hunan 410073, People's Republic of China

[a)]**Authors to whom correspondence should be addressed:** qimingze17@nudt.edu.cn and xjduan@nudt.edu.cn

ABSTRACT

Social distancing has been widely adopted to curb infectious disease outbreaks, but large-scale lockdowns and individual quarantines impose heavy social, psychological, and economic costs. This motivates the design of more sustainable, ego-centered contact-reduction strategies that operate at the individual level. In networks, distancing can be modeled by edge removal, but existing approaches rely on global topological information inaccessible to individuals. We assume behavioral changes are guided by local observations: each person selectively avoids contacts based on simple, locally accessible information. Inspired by weak-tie theory and the pronounced community structure of social networks, we propose a two-stage hybrid intervention whereby individuals first target low-degree neighbors for removal and subsequently eliminate ties with the fewest common neighbors. This ego-centered approach fragments community structures and isolates peripheral components, enabling effective epidemic suppression. Compared with strategies targeting highly connected nodes, our method achieves better outcomes while reducing social costs. These results highlight that interventions grounded in individual-level decisions and local tie information can inform practical social distancing policies without requiring global network knowledge.

Sustainable epidemic control requires strategies that guide individuals to reduce contact with others based on locally available information. Although complex networks are widely used to study such interventions, most existing approaches—such as network dismantling or targeted immunization—operate from a global perspective, identifying a minimal set of nodes or links whose removal most effectively fragments the entire network. In contrast, our framework adopts an ego-centered perspective: each person makes contact-reduction decisions using only local structural cues. Specifically, we examine a simple local metric—the number of common neighbors—and show that avoiding weak ties, rather than links to high-degree hubs, more effectively suppresses epidemic spread. This scalable approach leverages the community structure to mitigate disease spread in a socially sustainable manner, without requiring global information.

I. INTRODUCTION

Non-pharmaceutical interventions (NPIs), from case isolation to large-scale lockdowns, have been central to managing pandemics like COVID-19[1] and the H1N1 Influenza.[2] While effective, these measures impose significant societal burdens and require substantial administrative oversight, creating a need for sustainable strategies that balance viral containment with essential societal functions.[3–5] A promising direction lies in developing intervention policies that can be implemented at the individual level, empowering people to make informed distancing decisions using easily accessible, local information without depending on centralized directives or extensive surveillance.[6]

The effectiveness of such policies can be understood through the lens of network science, which models interactions as networks and epidemics as contagion processes upon them.[7–10] Interventions like social distancing function as processes of removing nodes (individuals) or links (interactions) to fragment the network and slow transmission.[11] Percolation theory has been widely used to clarify why interventions that change the contact network can alter epidemic tipping points and final epidemic size.[8] Network interventions often rank nodes or edges using centrality metrics such as degree,[12] closeness,[13] Katz,[14] collective influence,[15] and betweenness centrality[16]. Other studies target global structural indicators—such

as dismantling the giant connected component (GCC)[15,17] or adjusting the generalized Herfindahl–Hirschman index[18,19]—to inhibit epidemic spread. While many network intervention strategies effectively curb epidemics, they often rely on global information—such as identifying the most central individuals in the entire network—which is rarely available in real-time and raises privacy concerns.[15,18] This gap motivates the development of strategies that rely solely on local or uncompleted information, making them both practical and scalable.[20–24]

We focus on ego-centered network interventions that implement local disconnection mechanisms by establishing specific social rules or public health guidelines.[5,25] Each person selectively reduces contacts based on information available in their immediate neighborhood, without requiring complete network knowledge. Infection risk depends not only on the number of contacts but also on how those contacts interconnect. The number of common neighbors, measurable from an ego's local perspective, provides a proxy for tie strength and bridging potential, distinguishing redundant intra-community links from inter-community bridges. This principle echoes Granovetter's seminal "strength of weak ties" hypothesis, which identifies weakly embedded ties as critical for connecting otherwise disconnected communities.[26] In our model, ties with few common neighbors serve as a local proxy for such weak ties. If individuals could identify and temporarily remove such bridging ties based solely on local information, they could collectively disrupt global transmission pathways. The central challenge, therefore, is translating this sociological insight into a simple, locally executable rule for epidemic control.

Here, we design *hybrid* link-removal rules that prioritize edges with few common neighbors or connect to low-degree neighbors. Across both synthetic and empirical networks, these weak-tie–oriented heuristics, including the proposed *hybrid* rule, consistently suppress epidemic size and delay outbreaks using only local information. The results reveal that such local interventions fragment global connectivity by selectively dismantling inter-community bridges while preserving dense local clusters, validating the weak-tie principle in the context of epidemic control.

The main contributions of this study are as follows:

(1) **Ego-centered identification of weak ties.** We demonstrate that identifying and pruning weak ties based on local neighborhood information—requiring only the relational context among a node and its immediate contacts—effectively reduces outbreak size. This locally cooperative yet individually implementable mechanism provides a scalable approach to network intervention
(2) **Hybrid intervention design.** We propose a hybrid strategy integrating node degree and common-neighbor information, which achieves superior containment compared with strategies based on either metric alone.

The remainder of this paper is organized as follows. Section II introduces the problem setting and describes the ego-centered intervention strategies. Section III presents the simulation results and mechanistic analyses demonstrating how local weak-tie exclusion enhances containment through network modularization and fragmentation. Section IV concludes with a discussion of the broader implications for decentralized epidemic control and community-based public health strategies.

II. EGO-CENTERED NETWORK INTERVENTION BASED ON LOCAL STRUCTURAL INFORMATION

This section presents a framework for ego-centered interventions, including epidemic dynamics, problem formulation, and locally informed edge-removal strategies.

A. Problem formulation

We begin by introducing the epidemic models that form the basis of our intervention analysis. Disease propagation is simulated using the Susceptible–Infected–Recovered (SIR) and Susceptible–Infected–Susceptible (SIS) models,[27] implemented with synchronous updates. At each step, susceptible nodes are infected with probability β, and infected nodes recover with probability μ [Fig. 1(a)]. In SIR, recovered nodes remain immune, and the final outbreak size ρ_R quantifies the epidemic impact. In SIS, infections can recur, with steady-state prevalence ρ_I characterizing endemic levels. Unless otherwise stated, simulations are initialized with 1% of nodes randomly in the infected state and a recovery rate $\mu = 0.1$ is fixed, with results obtained by averaging over 10 000 independent realizations.

Social distancing interventions can be modeled as selective edge-removal processes on contact networks $G = (V, E)$, where individuals are represented as nodes and disease-transmitting contacts as edges. This transforms the original network into a perturbed version $G' = (V, E')$ with $E' \subset E$, on which epidemic dynamics are simulated. The effectiveness of such interventions is quantified by the reduction in outbreak size ρ_R (for SIR models) or steady-state prevalence ρ_I (for SIS models) in G' compared to G [Fig. 1(a)].

Unlike global strategies that rank and remove edges from the entire network E based on complete topological knowledge, our **ego-centered intervention model** operates under limited information. Each node i can only observe its local neighborhood and independently decides to disconnect a fraction p of its direct edges $(i, j) \in E_i$ based on local information or the structural properties of its neighbors, such as their degree or the number of common neighbors between i and j, as illustrated in Fig. 1(b). The parameter p represents the intervention intensity, analogous to the strength of social distancing adoption. In real-world settings, the information needed for our model is readily available through multiple channels. Digital platforms like Facebook provide direct measures of neighbor degree and common neighbors via friend lists and mutual connections—such metrics could be incorporated into privacy-preserving contact-tracing applications. Similarly, organizational charts reveal connection patterns in work environments. Even without digital tools, individuals can often infer common neighbors and estimate a contact's degree through ordinary social interaction.

Each vertex ranks its neighbors according to specific criteria—such as ascending order of common neighbors or descending order of neighbor degree [Fig. 1(c)]—and selectively removes a fraction of the highest-ranked connections. The objective is to minimize epidemic spread using only ego-centered information. Formally, the

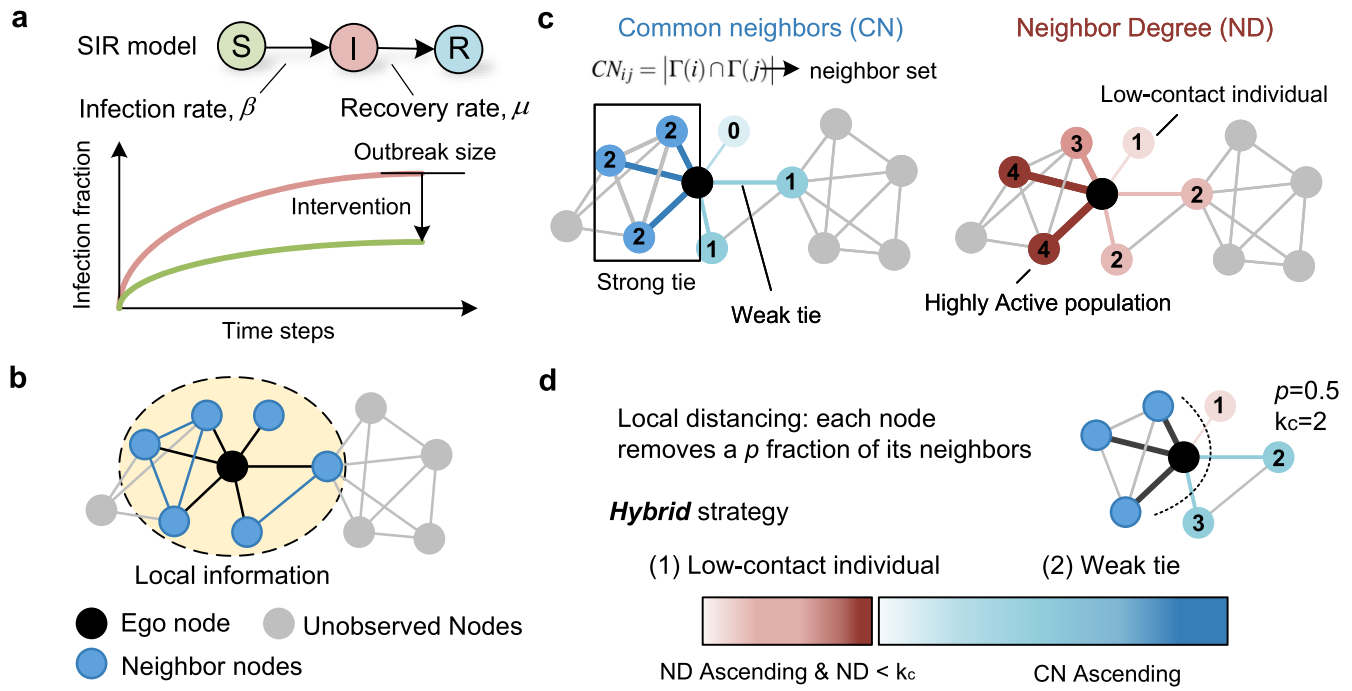

FIG. 1. Limited information guiding local protective decisions. (a) A susceptible–infected–recovered (SIR) model with infection (β) and recovery (μ) rates simulates epidemic spread; interventions aim to minimize the final outbreak size. (b) An ego node (black) determines which connections to retain or remove by observing its local neighborhood, including ties among its peers. (c) Two local metrics are employed: common neighbors (CN) quantify tie strength, with links having fewer shared neighbors interpreted as weaker ties, whereas neighbor degree (ND) characterizes contact activity, separating low-contact from highly active individuals. (d) Local distancing removes a fraction p of each node neighbor according to these metrics. The hybrid strategy first disconnects low-degree neighbors (ND ascending, ND $< k_c$) and then weak ties (CN ascending).

problem can be expressed as

$$\begin{aligned} \min_{E' \subseteq E} \quad & \rho_R(G'), \\ \text{s.t.} \quad & |\mathcal{R}_i| \le \lfloor pk_i \rfloor, \quad \forall i \in V, \\ & \mathcal{R}_i = \mathcal{F}_i\left(\{(k_j, C_{ij}) : j \in \Gamma(i)\}\right), \\ & E' = E \backslash \bigcup_{i \in V} \mathcal{R}_i, \end{aligned} \tag{1}$$

where for each node $i \in V$, the removal set $\mathcal{R}_i \subseteq E_i$ is determined by a local decision function $\mathcal{F}_i$, which takes as input the set of neighbor features [e.g., degrees k_j and common neighbor counts C_{ij} for all $j \in \Gamma(i)$] and the removal fraction p. The function $\mathcal{F}_i$ outputs a ranking of edges in E_i, from which the top-$\lfloor pk_i \rfloor$ edges are selected for removal. By progressively pruning edges based on neighborhood-level information, we generate an edge-percolation process that models incremental local distancing and examines how simple, locally informed strategies reshape epidemic spread and the network structure.

1. Local structural metrics

Consider an undirected network $G = (V, E)$, where node i has degree k_i. Ego-centered interventions use neighborhood-level structural metrics accessible to each individual:

Neighbor degree (k_j): The degree of neighbor j. High-degree neighbors are local hubs, while low-degree neighbors are more peripheral.[28]

Common neighbors (CN_{ij}) is used as a structural proxy for tie strength; low CN_{ij} indicates weak ties, which—according to Granovetter's theory—are more likely to act as bridges connecting different densely knit social circles (communities).[29] This makes them critical for global connectivity and, consequently, for epidemic spread. For adjacent nodes i and j, the number of common neighbors is

$$CN_{ij} = |\Gamma(i) \cap \Gamma(j)|, \tag{2}$$

where $\Gamma(i)$ denotes the set of neighboring nodes for i. Weakly embedded connections (with low CN) often serve as bridges between densely knit social circles. Here, we use the number of common neighbors as a structural proxy for the strength of a social tie. Although the number of common neighbors requires limited second-order neighborhood information, this remains observable within an egos local social context (e.g., awareness of whether two friends know each other).

Neighbor betweenness (B_j): The betweenness centrality of neighbor j, measuring its role in mediating shortest-path flow across

the network,[16,30]

$$B_j = \sum_{s \neq t} \frac{\sigma_{st}(j)}{\sigma_{st}}, \tag{3}$$

where σ_{st} is the total number of shortest paths from node s to node t, and $\sigma_{st}(j)$ counts those passing through j. High betweenness identifies nodes that act as brokers or bridges controlling global flow. Since its calculation requires knowledge of the entire network, B_j serves primarily as a benchmark rather than a locally implementable metric.

These metrics capture complementary aspects of the network structure relevant to epidemic spread: edges with few common neighbors represent the weak ties that bridge communities and facilitate long-range transmission, peripheral nodes link sparsely connected clusters, and high-betweenness nodes act as brokers mediating flow along shortest paths. Building on this formulation, we next develop a hybrid mechanism that operationalizes the intervention using only locally accessible information.

B. Hybrid intervention strategy via weak-tie exclusion

Single-metric heuristics may have drawbacks. For instance, exclusively targeting weak ties might miss vulnerable peripheral nodes, while targeting low-degree nodes might preserve powerful inter-community bridges if they happen to involve high-degree individuals. To overcome these limitations, we propose a hybrid strategy that synergistically combines degree and common-neighbor information [Fig. 1(d)].

The hybrid strategy partitions a node is neighbors based on a local degree threshold, $k_c = \alpha \langle k(\Gamma(i)) \rangle$, where $\langle k(\Gamma(i)) \rangle$ is the average degree of is neighbors and α is a tunable coefficient. We set $\alpha = 0.3$, which provides a favorable trade-off between epidemic suppression and edge preservation (see Appendix B for details). The removal logic follows a two-stage process:

(1) Peripheral isolation. For neighbors with a degree below the threshold ($k_j < k_c$), the strategy targets them for disconnection. Edges are ranked in ascending order of the neighbor's degree (k_j). The goal of this phase is to prune the most peripheral, weakly attached nodes first, effectively quarantining the network's extremities to prevent them from acting as entry points for infection.

(2) Core bridge-breaking. For neighbors with a degree at or above the threshold ($k_j \geq k_c$), the focus shifts from the node itself to the nature of the tie. Edges are ranked in ascending order of common neighbors. This phase aims to identify and sever the weak, non-redundant ties connected to the more central players in the local neighborhood. By breaking these "bridges," the strategy disrupts critical pathways for long-range disease transmission that might otherwise traverse the network's core.

This dual approach establishes a ranking of edges for removal: ties to neighbors with degrees below the threshold are pruned first, sorted by ascending degree. Subsequently, ties to remaining neighbors are pruned, sorted by ascending number of common neighbors. It simultaneously targets two distinct types of vulnerabilities: isolating peripheral actors and dismantling the weak ties that connect influential ones, leading to a more robust and effective epidemic mitigation performance.

C. Benchmark heuristics for comparison

To evaluate the effectiveness of our hybrid strategy, we compare it against several baseline heuristics that rely on a single metric. As a null model, a **random** removal strategy is used, where each individual disconnects a random fraction of contacts, representing untargeted social distancing.

1. Common-neighbor strategies

The *low common neighbor* (CNL) strategy removes edges in ascending order of C_{ij}. CNL preferentially removes weak ties, which often serve as inter-community bridges, thereby fragmenting the network while preserving local clusters. Its inverse, *high common neighbor* (CNH), removes edges in descending order of C_{ij}, deliberately disrupting dense intra-cluster connections that represent strong, redundant relationships.

2. Degree-based strategies

The *low neighbor degree* (NDL) strategy removes edges attached to low-degree neighbors, typically peripheral nodes, preventing outbreaks from reaching the network core. Its inverse, *high neighbor degree* (NDH), targets highly connected neighbors, akin to intervening on super-spreaders.

3. Betweenness-based strategies

The *low neighbor betweenness* (NBL) strategy targets edges to neighbors with low betweenness, affecting locally embedded ties. The reverse, *high neighbor betweenness* (NBH), removes edges to high-betweenness neighbors, disrupting brokers that mediate global flow. As betweenness requires global knowledge, NBH and NBL serve as benchmarks rather than locally implementable strategies.

These heuristics exploit structural cues relevant to epidemic control: weak ties facilitate long-range spread, peripheral nodes maintain hidden bridges, and brokers regulate network flow. They emulate real-world behaviors such as avoiding casual acquaintances, limiting exposure to hubs, or disrupting key conduits during outbreaks.

III. EXPERIMENTAL ANALYSIS

A. Performance on synthetic networks

To assess how local distancing interventions mitigate epidemics, we examine edge-removal strategies that use only neighborhood information to interrupt transmission pathways. We hypothesize that selectively cutting weak inter-community ties—rather than targeting high-centrality nodes—may more effectively fragment networks and limit disease spread. To test this idea, we implement a family of locally informed edge-removal strategies, including the removal of weak acquaintance links (CNL) or the avoidance of highly connected neighbors (NDH), and progressively removing a fraction p of edges to create an edge-percolation process that models incremental local distancing.

We evaluate these strategies on three synthetic community networks—Lancichinetti–Fortunato–Radicchi (LFR),[31] Kumpula–Onnela–Saramäki–Kaski–Kertész (KOSKK),[32,33] and stochastic block

model (SBM) networks.[34,35] Network details are given in the Appendix, with structural properties summarized in Table I. Outbreak size decreases as the neighbor removal fraction p increases (Fig. 2). In tested networks, strategies targeting neighbors with few common neighbors (CNL, hybrid) generally outperform high-centrality approaches under both high ($\beta = 0.25$) and low ($\beta = 0.05$) infection rates. However, these performance differences become less significant in networks with weaker modularity. At lower infection rates, CNL yields the greatest suppression by trapping transmission within communities. At higher infection rates, NDL is more efficient at low removal fractions ($p < 0.2$), suggesting that disconnecting from peripheral, low-degree neighbors is cost-effective against more transmissible pathogens, although the advantage diminishes as p increases. The *hybrid* strategy—first removing

TABLE I. Topological properties of the studied networks. Key metrics include the number of nodes (N) and edges (W); epidemic threshold ($T_c = \langle k \rangle / \langle k^2 \rangle$), where $\langle k \rangle$ and $\langle k^2 \rangle$ represent the first and second moments of the degree distribution, respectively, and the average clustering coefficient C. Q represents the modularity measure, with community structures identified using the Louvain algorithm.[37]

Network	N	W	$\langle k \rangle$	T_c	C	Q
LFR	1000	5669	11.34	0.058	0.21	0.73
SBM	1000	4299	8.59	0.106	0.06	0.70
KOSKK	1000	4474	8.95	0.060	0.553	0.698
Politic Blog	1222	16714	27.36	0.012	0.320	0.4252
Facebook	362	1988	10.98	0.046	0.58	0.67
Football	115	613	10.66	0.09	0.40	0.60

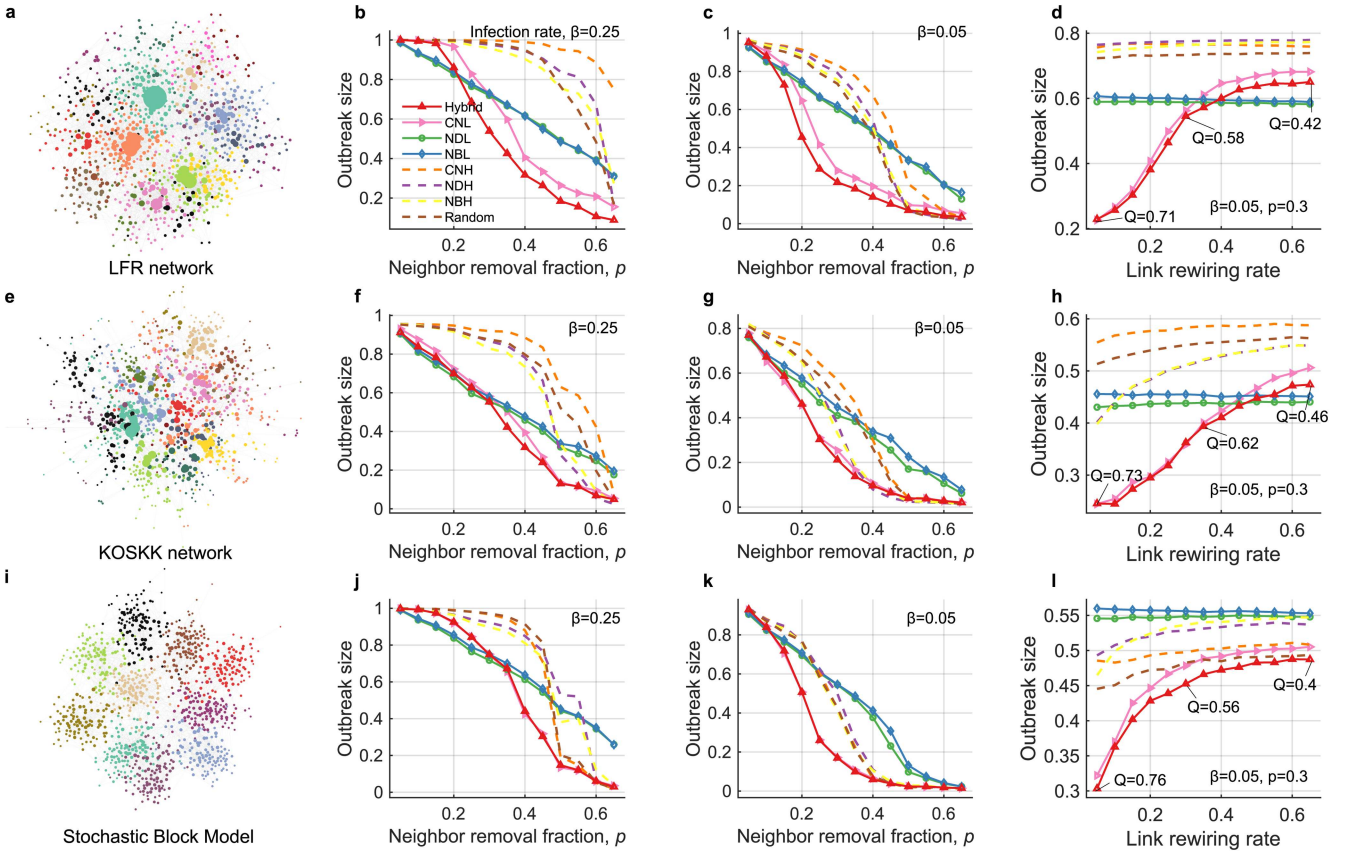

FIG. 2. Performance of ego-centered intervention strategies in synthetic community networks. (a), (e), and (i) Visualizations of the Lancichinetti–Fortunato–Radicchi (LFR), Kumpula–Onnela–Saramäki–Kaski–Kertész (KOSKK), and Stochastic Block Model (SBM) networks, respectively, with colors indicating distinct communities. (b), (c), (f), (g), (j), and (k) Final outbreak size as a function of fraction of removed links (p) under different intervention strategies. These panels compare performance for a high infection rate ($\beta = 0.25$, left column) and a low infection rate ($\beta = 0.05$, middle column). Strategies include removing links with ascending common neighbors (CNL), ascending neighbor degree (NDL), ascending neighbor betweenness (NBL), and their descending-order counterparts (CNH, NDH, NBH). The random removal strategy serves as a baseline. Notably, strategies that remove links in ascending order (CNL, NDL, NBL) typically yield smaller outbreak sizes than their descending-order counterparts across the diverse network types and infection rates studied here. (d), (h), and (l) Final outbreak size as a function of link rewiring rate, where degree-preserving randomization is performed to reduce network modularity Q. The parameters are fixed at $\beta = 0.05$ and $p = 0.3$.

edges incident to low-degree nodes and then applying the CNL criterion—achieves performance comparable to or slightly better than CNL under all tested conditions. In contrast, strategies targeting high-metric edges yield limited benefit because such edges typically lie within densely interconnected modules.

Building on these comparative results, we identify a general structural pattern: under our test networks, strategies prioritizing links with low metric values (L-strategies: CNL, NDL, NBL) are substantially more effective than those focusing on high metric values (H-strategies: CNH, NDH, NBH). Removing links with the fewest common neighbors, for example, significantly curtails outbreaks, whereas removing those with the most common neighbors performs only slightly better than random removal. These findings provide mechanistic support for Granovetter's hypothesis within an epidemic context: preferentially removing weakly embedded ties (low CN), which often act as inter-community bridges, is highly effective at fragmenting the network and containing outbreaks.

To directly test whether community fragmentation drives these differences, we systematically reduced network modularity through degree-preserving randomization [Figs. 2(d), 2(h), 2(l)]. This technique maintains the original degree sequence while randomly selecting pairs of edges (A, B) and (C, D) to rewire them as (A, D) and (C, B), with this process repeated multiple times to generate randomized topologies.[36] This approach destroys the community structure, clustering, and assortativity, allowing us to analyze the impact of modularity on our strategy. As modularity decreases, the protective advantage of CNL and *hybrid* strategies declines proportionally, confirming that their effectiveness depends on exploiting weak inter-community connections. Although degree-preserving randomization erodes the structural features that these local strategies target, high-centrality approaches remain largely unaffected, consistent with their focus on core-embedded links.

Having established that community structure is a key determinant of our strategies' success, we next investigate how their performance profiles vary across a broad spectrum of epidemiological conditions by simulating various infection rates (β) and neighbor removal fractions (p). Phase diagrams of final outbreak sizes on LFR networks [Figs. 3(a)–3(d)] reveal distinct containment profiles across strategies. The *hybrid* strategy effectively suppresses outbreaks across the entire parameter space, maintaining an extensive low-prevalence region. This advantage persists in both moderate ($p = 0.3$) and aggressive ($p = 0.5$) interventions, where *hybrid* strategy yields the smallest outbreak sizes across a broad range of infection rates [Figs. 3(e) and 3(f)]. NDL performs best for highly contagious pathogens ($\beta > 0.2$) when interventions are limited ($p < 0.3$), whereas NDH consistently produces larger outbreaks. These findings indicate that strategies prioritizing the disconnection of peripheral nodes and clusters are more effective than targeting higher-degree connections. The superior performance of the *hybrid* approach can be attributed to its dual-phase mechanism. The initial phase involves the removal of low-degree nodes, a process that safeguards sparsely connected individuals. This is followed by a subsequent elimination stage based on ascending common-neighbor counts, a process that is intended to impede inter-community transmission.

To isolate the effect of removal order, we compare the ascending-order (L) and descending-order (H) implementations of the same heuristics—common neighbors (CN), neighbor degree (ND), and neighbor betweenness (NB). Phase diagrams and

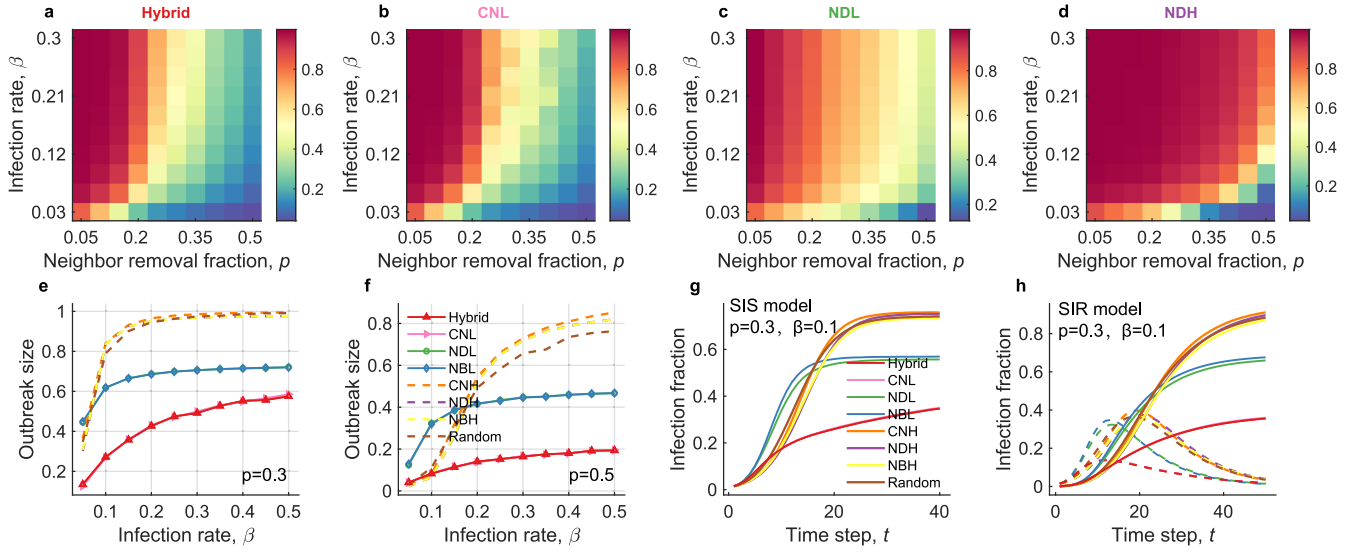

FIG. 3. Effectiveness of ego-centered intervention strategies across infection rates. (a)–(d) Phase diagrams of final SIR outbreak size as a function of infection rate (β) and neighbor removal fraction (p) for the *hybrid*, CNL, NDL, and NDH strategies. Cooler colors indicate a stronger containment. (e)–(f) Outbreak size vs infection rate at fixed removal ratios $p = 0.3$ and $p = 0.5$. (g)–(h) Temporal evolution of infection prevalence for $p = 0.3, \beta = 0.1$ under the SIS (g) and SIR (h) models. Solid curves represent the ascending (low-to-high) rules, and dashed curves represent the reverse (high-to-low) rules.

temporal infection curves [Figs. 3(g) and 3(h)] reveal a consistent pattern: ascending-order removal invariably yields smaller final outbreaks and a relatively slower growth trend than the corresponding descending-order strategy. This systematic advantage underscores a principle of prioritizing the disconnection of peripheral nodes and weakly embedded ties. We term this the "peripheral isolation" principle. As shown by our structural analysis (Fig. 4), by first removing peripheral and weakly connected links, these strategies rapidly increase network modularity [Fig. 4(f)] and selectively prune inter-community links [Fig. 4(e)]. This effectively compartmentalizes the network, trapping the contagion within disconnected, dense clusters before it can achieve global reach. In contrast, attacking the core first leaves these peripheral bridges intact, facilitating widespread diffusion. This approach is computationally cheaper and more effective when using local information than directly attacking the core, which is often more globally embedded and harder to protect through social distancing. This intriguing result also implies that misguided interventions, which intuitively target highly active individuals, might inadvertently preserve critical bridges and, thus, lead to significantly poorer outcomes, in some cases performing only marginally better than random removal.

B. Structural mechanisms underlying intervention efficacy

To elucidate the structural mechanisms responsible for these different containment outcomes, we quantify the size of the giant connected component (GCC) as edges are removed and visualize the residual topology at a removal fraction of $p = 0.3$ on the LFR network [Figs. 4(a)–4(d)]. In the LFR network, the *hybrid* strategy produces the most rapid decline of the giant connected component (GCC), with collapse observed near $p \approx 0.35$ in our simulations, earlier than for the other tested strategies. CNL exhibits a similar but slightly weaker effect, highlighting the efficiency of targeting ties with a few common neighbors. Visual inspection of the remaining network [Fig. 4(b)] reveals numerous small, densely knit clusters, consistent with the rapid decline of the inter-community ratio [Fig. 4(e)], rising modularity [Fig. 4(f)], and the peak in clustering at intermediate p [Fig. 4(g)]. These patterns indicate that pruning peripheral low-degree nodes followed by ascending removal of weakly embedded neighbors efficiently dismantles large-scale connectivity.

To evaluate whether this rapid fragmentation is unique to common-neighbor targeting, we next examine degree- and betweenness-based removals. NDL shrinks the giant connected component (GCC) smoothly, leaving a compact hub-dominated core and numerous isolated nodes at comparable removal fractions [Fig. 4(c)]. Meanwhile, NBL produces only a slightly faster decline. Reverse strategies (dashed lines) demonstrate the opposite pattern: eliminating neighbors with high common-neighbor, degree, or betweenness scores (CNH, NDH, NBH) preserves connectivity far longer. Additionally, the heterogeneity of network degree values significantly decreases, with most nodes exhibiting similar degree values [Fig. 4(d)].

Beyond global connectivity, mesoscopic community structure critically shapes epidemic spread. We, therefore, measure

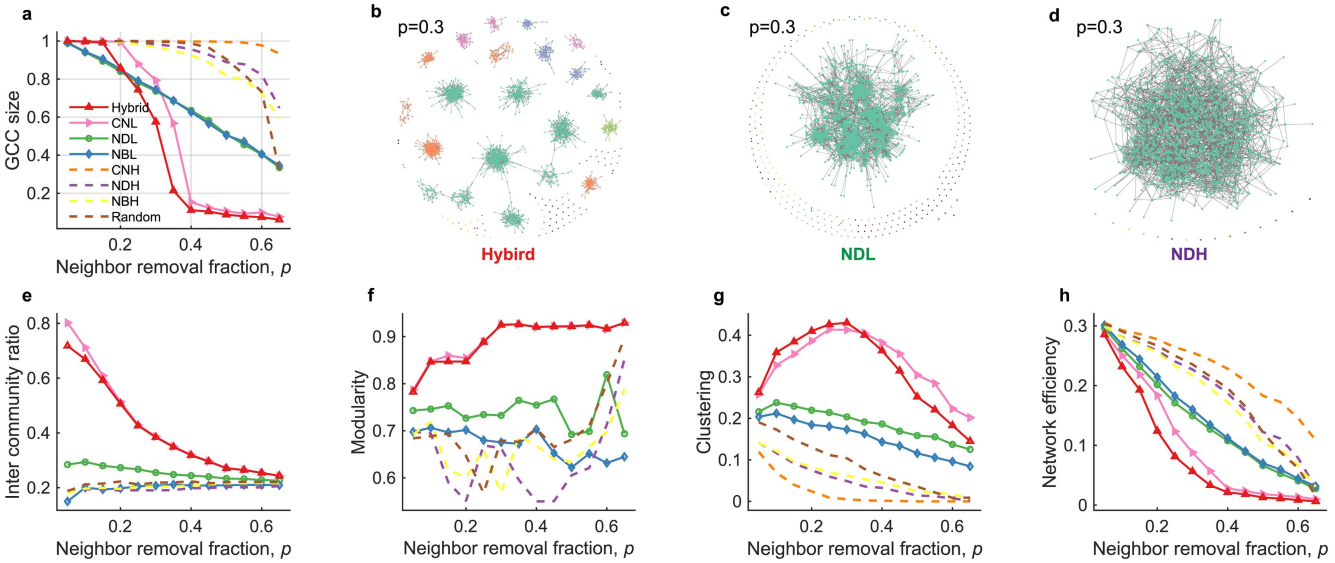

FIG. 4. Structural impact of ego-centered intervention strategies on the LFR network. (a) Relative size of the giant connected component (GCC) as a function of neighbor–removal fraction p. (b)–(d) Representative network realizations at $p = 0.3$ under three typical strategies (*hybrid*, NDL, and NDH), highlight the contrasting fragmentation patterns. (e)–(h) Evolution of inter-community ratio, modularity, clustering coefficient, and network efficiency with increasing removal fraction. Solid curves correspond to the ascending (L-strategies like CNL and NDL) rules, while dashed curves represent the descending (H-strategies like CNH and NDH) rules. Note how L-strategies lead to a faster GCC collapse (a), a sharper increase in modularity (f), and a more significant drop in network efficiency (h), all of which are indicative of effective epidemic containment through network fragmentation.

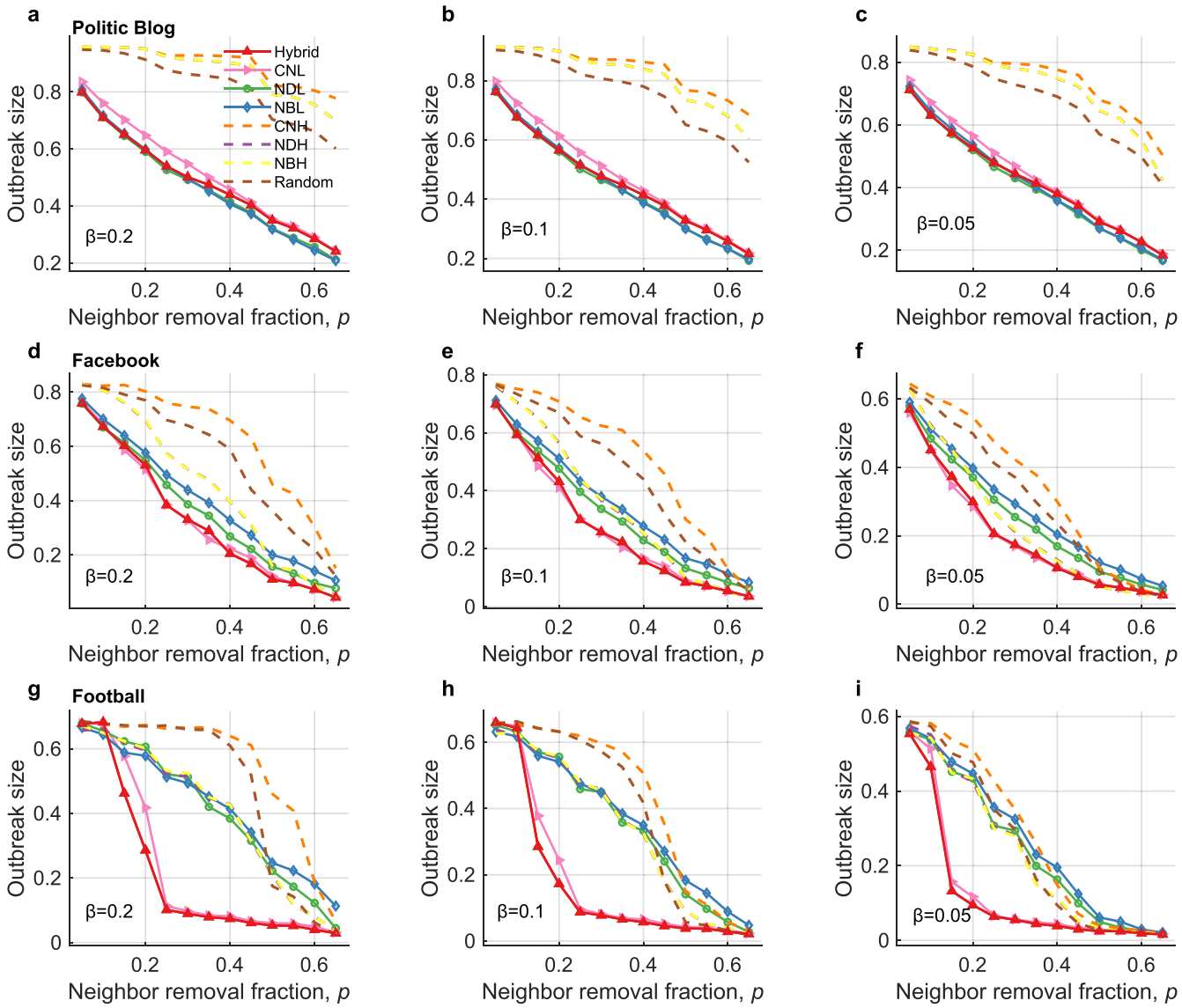

FIG. 5. Ego-centered intervention strategies for epidemic mitigation in real social networks. Comparative analysis across three empirical networks: Politic Blog (a)–(c), Facebook (d)–(f), and Football (g)–(i). The panels show the final outbreak size vs neighbor removal fraction (p) at varying infection rates ($\beta = 0.05, 0.1, 0.2$), demonstrating the efficacy of targeted intervention strategies for different network topologies.

the fraction of inter-community links removed and the residual modularity Q [Figs. 4(e) and 4(f)]. *Hybrid* and CNL remove more inter-community bridges than competing strategies, producing networks of markedly higher modularity. This demonstrates that these approaches compartmentalize the network by severing global bridges, a mechanism that limits cross-community transmission. Having established their effects on global and mesoscopic scales, we finally assess local clustering and global efficiency [Figs. 4(g) and 4(h)]. Ascending-order strategies—particularly *hybrid* and CNL—induce the steepest declines in network efficiency, eliminating redundant pathways and slowing epidemic spread.

The efficacy of the hybrid rule is attributable to its dual application of complementary dismantling mechanisms: Peripheral isolation, which targets THE nodes connected to low-degree neighbors. In contrast, core bridge-breaking focuses on nodes that serve as critical links between dense communities. The peripheral component

is notably efficient; by disconnecting vulnerable neighbors with minimal redundant paths to the main network, it enables rapid fragmentation of the network's periphery and increases the number of disconnected components. In contrast, the core bridge component addresses essential nodes that sustain network connectivity. Although these nodes are typically well-connected and, thus, more costly to isolate, their removal cleaves the network, disrupting connections between major clusters. Our hybrid approach effectively combines both mechanisms, resulting in a more rapid and comprehensive collapse.

C. Validation on empirical networks

To validate the principles derived from these idealized models in more complex and realistic settings, we apply the same strategies to several empirical networks, including Political Blog, Facebook, and Football (see Table I).

We specifically focus on three empirical networks with diverse topologies: the Political Blog network, the Facebook friendship network, and the Football network. For each, we measure final outbreak size as a function of neighbor removal fraction under different infection rates (Fig. 5). Across all scenarios, the *hybrid* strategy tends to yield the smaller outbreaks, suggesting that sequentially targeting peripheral nodes before removing weakly connected members provides a broadly applicable and robust containment approach. In real-world networks, the strategies prioritizing the removal of edges connected to neighbors with low common neighbors (CNL), low degree (NDL), and low betweenness (NBL) significantly outperform their high-centrality counterparts (CNH, NDH, and NBH). This counter-intuitive finding suggests that severing "weak ties" to structurally less important neighbors is a more potent method for halting epidemics than disconnecting from local hubs. These weak links may act as critical bridges for the pathogen to spread between different communities or denser regions of the network.

The advantage of the *hybrid* strategy persists across networks with different structural characteristics. In the highly clustered Facebook network [Figs. 5(d)–5(f)], *hybrid* maintains the smallest outbreak size even at low transmissibility ($\beta = 0.05$), while in the community–rich Football network [Figs. 5(g)–5(i)], it reduces outbreaks by more than 50% compared with other targeted strategies under high transmissibility ($\beta = 0.2$). These results demonstrate that *hybrid*'s two-stage design reliably disrupts both macro-scale connectivity and mesoscopic community structure, enabling robust epidemic control across diverse real-world systems.

IV. CONCLUSION AND DISCUSSION

Our investigation demonstrates that a family of locally informed distancing strategies, which require only ego-centered network information, can effectively suppress epidemic spread. The efficacy of the CNL and hybrid strategies stems from a key principle: removing weakly embedded ties (low CN) fragments the network by dismantling inter-community bridges. This structural mechanism is the cornerstone of our approach. It operationalizes Granovetter's "strength of weak ties" theory, suggesting that these sociologically defined weak links can also be crucial for epidemic control. By preferentially severing links that connect distinct modules, the CNL and hybrid strategies induce a rapid increase in network modularity and a precipitous drop in the size of the giant connected component. This intervention effectively traps the contagion within isolated, dense clusters, preventing global outbreaks.

The practical implications of our findings are significant. They suggest that public health guidance could be refined to focus not only on the number of contacts but also on their type, encouraging the minimization of contacts with acquaintances who are not well-integrated into one's own social circle. This approach is inherently scalable and could, in principle, be privacy-preserving, as it relies on information individuals can readily access without necessarily requiring centralized surveillance. It is particularly well-suited for implementation in digital social platforms or organizational settings where local network information can be easily approximated.

However, the effectiveness of our proposed strategies is contingent upon several factors. First, our model operates on a static network snapshot. Future work should explore performance in adaptive coevolutionary models, where link removal and epidemic dynamics interact. This co-evolutionary dynamic may lead to emergent phenomena, such as the spontaneous formation of resilient, isolated communities, or conversely, the accelerated collapse of social cohesion under intervention pressure. Second, we assume perfect adoption of the distancing strategy. The effectiveness under varying levels of compliance, modeled using game-theoretic frameworks, is a crucial next step. Third, our model treats all contacts as binary. Investigating the correlation between our topological proxy (common neighbors) and interaction frequency (edge weight) is essential for translating these findings into practical advice.

Despite these limitations, our work provides a foundational framework for designing decentralized, resource-efficient network interventions. This work contributes to a growing shift in focus from interventions requiring global topology to those leveraging local intelligence. In conclusion, our work demonstrates that local network interventions, guided by the simple heuristic of removing weak ties, are a potent strategy for containing epidemic spread. This approach efficiently fragments the network into disconnected communities, halting large-scale transmission. Our findings bridge sociological theory with network epidemiology, providing a formal basis for the intuition that weakening the network's "bridges" is more effective than attacking its "hubs" when only local information is available. This research opens several avenues for future work toward a new class of intervention strategies that balance efficacy with practical constraints like scalability and privacy.

ACKNOWLEDGMENTS

Mingze Qi and Xiaojun Duan are supported by the National Natural Science Foundation of China (NSFC) (Nos. 72401290 and U2230208), the Major Scientific and Technological Innovation Platform Project of Hunan Province (No. 2024JC1003), and the Hunan Science and Technology Plan Project (No. 2025JJ50417). Xin Lu is supported by the National Natural Science Foundation of China (NSFC) (Nos. 72025405, 72421002, and 92467302), and the Major Program of Xiangjiang Laboratory (No. 24XJJCYJ01001).

AUTHOR DECLARATIONS

Conflict of Interest

The authors have no conflicts to disclose.

Author Contributions

Peng Chen: Conceptualization (equal); Data curation (equal); Formal analysis (equal); Methodology (equal); Software (equal); Validation (equal); Visualization (equal); Writing – original draft (equal); Writing – review & editing (equal). **Mingze Qi:** Conceptualization (equal); Formal analysis (equal); Methodology (equal); Software (equal); Validation (equal); Visualization (equal); Writing – review & editing (equal). **Zhi Zeng:** Validation (supporting); Writing – review & editing (supporting). **Xiaojun Duan:** Conceptualization (equal); Formal analysis (equal); Methodology (equal); Writing – review & editing (equal). **Xin Lu:** Conceptualization (equal); Formal analysis (equal); Methodology (equal); Writing – review & editing (equal).

DATA AVAILABILITY

The data that support the findings of this study are available from the corresponding authors upon reasonable request.

APPENDIX A: MODEL NETWORKS

1. LFR benchmark networks

The LFR benchmark model[31] generates synthetic networks with power-law degree and community-size distributions, $P(k) \sim k^{-\gamma_1}$ and $P(c) \sim c^{-\gamma_2}$, capturing the coexistence of heterogeneous hubs and pronounced community structure typical of social systems. We generate networks with $N = 1000$ nodes, degree exponent $\gamma_1 = 3$, community-size exponent $\gamma_2 = 1.5$, average degree $\langle k \rangle = 10$, minimum community size $c_{\min} = 20$, and a mixing parameter $\tau = 0.1$, such that approximately 10% of each node connection extends beyond its own community. The degree and community-size sequences are sampled self-consistently, with invalid instances resampled until all constraints are satisfied. All networks are unweighted, although weights can be later assigned if required for dynamical simulations. The low mixing parameter ensures strong modularity—dense intra-community connections bridged by a small number of high-degree nodes—mimicking real social systems in which a few central individuals connect otherwise tightly knit groups.

2. KOSKK networks

The KOSKK model[32,33] generates social networks through a dynamic triadic-closure process that reinforces existing ties and drives community formation. The model starts with $N = 1000$ isolated nodes, and all new edges are assigned an initial weight $w_0 = 1$.

a. Local attachment

A node v_j is chosen at random, and one of its neighbors v_k is selected with probability $\omega_{jk} / \sum_k \omega_{jk}$, where ω_{jk} denotes the weight of link e_{jk}. If v_k has additional neighbors, one of them, v_l, is chosen with probability $\omega_{kl} / \sum_l (\omega_{kl} - \omega_{jk})$. If no link exists between v_j and v_l, a new edge is added with probability $p_\Delta = 0.25$ and weight $w_0 = 1$. Each interaction increases the involved link weights by $\delta = 0.6$.

b. Global attachment

With probability $p_r = 0.005$, node v_j connects to a random node (or with probability 1 if v_j is isolated), and the new link is assigned weight $w_0 = 1$.

c. Node deletion

A randomly selected node loses all its connections with probability $p_d = 0.001$.

The dynamics proceed for $T = 10^7$ update steps, after which the network reaches statistical stationarity in key observables such as average degree and clustering coefficient. The resulting networks exhibit high clustering, broad but non–scale-free degree distributions, and densely overlapping cliques feature the emblematic of cohesive social structures such as families, workplaces, and local communities.

d. Stochastic block model (SBM) networks

SBM networks[34,35] provides a generative framework for networks with explicitly defined modular organization and homogeneous within-group density. We construct SBM networks with $N = 1000$ nodes partitioned into $B = 10$ equal-sized communities of $n_i = 100$ nodes each. To achieve a target average degree of $\langle k \rangle = 8$, intra-community edges are created with probability $p_{\text{in}} = \langle k \rangle / (n_i - 1)$, while inter-community edges occur independently with probability $p_{\text{out}} = 10^{-4}$. This configuration produces strongly modular structures with dense intra-group connections and sparse inter-group bridges, analogous to organizations with distinct departments or classrooms with balanced internal interactions.

APPENDIX B: PARAMETER SENSITIVITY OF THE HYBRID STRATEGY

The definition of the hybrid strategy in Section II B is governed by the parameter α, which balances peripheral isolation against core bridge-breaking. To validate our selection of $\alpha = 0.3$ and evaluate the robustness of the method, we conduct a parameter sensitivity analysis by varying α from 0 to 0.9. The performance is assessed on two distinct network topologies: LFR networks with pronounced community structures and PB networks characterized by a dense, hard-to-separate core.

Figure 6 presents the sensitivity analysis, revealing distinct performance patterns for the hybrid strategy across different α values in the two networks. In the LFR network, strategies with α values in the range of 0.1–0.3 demonstrate superior effectiveness in containing the outbreak size, as shown in Fig. 6(a). This is attributed to the strategy's ability to effectively exploit the clear community structure by targeting inter-community connections. However, a pure core-breaking approach ($\alpha = 0$) may exhibit slower fragmentation in the initial phase compared to the hybrid strategy, as it might overlook easily removable peripheral nodes, potentially reducing its initial efficiency.

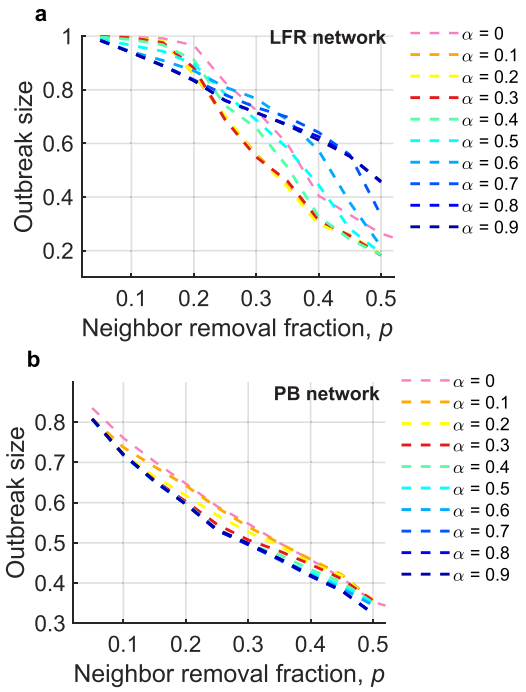

FIG. 6. Sensitivity analysis of the hybrid strategy parameter α. The outbreak size as a function of neighbor removal fraction for the hybrid strategy on LFR (a) and PB networks (b). Each curve represents a distinct value of α, varying from 0.0 to 0.9.

Conversely, in the PB network with its resilient dense core, strategies with higher α values (e.g., $\alpha \to 1$, approaching a pure peripheral isolation) led to better performance, as illustrated in Fig. 6(b). Low α strategies can cause rapid initial network fragmentation. However, because the connections within the dense core remain largely intact, further collapse of the network becomes increasingly difficult, limiting the overall effectiveness of the strategy.

Our findings show that a balanced approach delivers superior performance, effectively containing outbreak size when α ranges from approximately 0.2 to 0.4. This demonstrates that our choice of $\alpha = 0.3$ is not arbitrary—it represents a compromise that effectively integrates both fragmentation mechanisms for robust performance.

REFERENCES

[1]R. J. Glass, L. M. Glass, W. E. Beyeler, and H. J. Min, "Targeted social distancing designs for pandemic influenza," Emerging Infect. Dis. **12**, 1671 (2006).
[2]S. Etemad, I. Avci, P. Kumar, D. Baleanu, and S. Rezapour, "Some novel mathematical analysis on the fractal–fractional model of the AH1N1/09 virus and its generalized Caputo-type version," Chaos Soliton. Fract. **162**, 112511 (2022).
[3]H. Zhou, Q. Zhang, Z. Cao, H. Huang, and D. Dajun Zeng, "Sustainable targeted interventions to mitigate the COVID-19 pandemic: A big data-driven modeling study in Hong Kong," Chaos **31**, 101104 (2021).
[4]D. Meidan, N. Schulmann, R. Cohen, S. Haber, E. Yaniv, R. Sarid, and B. Barzel, "Alternating quarantine for sustainable epidemic mitigation," Nat. Commun. **12**, 220 (2021).
[5]P. Block, M. Hoffman, I. J. Raabe, J. B. Dowd, C. Rahal, R. Kashyap, and M. C. Mills, "Social network-based distancing strategies to flatten the COVID-19 curve in a post-lockdown world," Nat. Hum. Behav. **4**, 588–596 (2020).
[6]S. Chang, E. Pierson, P. W. Koh, J. Gerardin, B. Redbird, D. B. Grusky, and J. Leskovec, "Mobility network models of COVID-19 explain inequities and inform reopening," Nature **589**, 82–87 (2021).
[7]M. E. J. Newman, A. L. Barabási, and D. J. Watts, *The Structure and Dynamics of Networks* (Princeton University Press, 2006).
[8]R. Pastor-Satorras, C. Castellano, P. V. Mieghem, and A. Vespignani, "Epidemic processes in complex networks," Rev. Mod. Phys. **87**, 925–979 (2015).
[9]X. Lu, J. Feng, and S. Tan, "Perspectives on modelling epidemics with human mobility," Europhys. Lett. **149**, 41002 (2025).
[10]X. Lu, J. Feng, S. Lai, P. Holme, S. Liu, Z. Du, X. Yuan, S. Wang, Y. Li, X. Zhang, Y. Bai, X. Duan, W. Mei, H. Yu, S. Tan, and F. Liljeros, "Human mobility in epidemic modeling," arXiv:2507.22799 [cs.SI] (2025).
[11]H. He, H. Deng, Q. Wang, and J. Gao, "Percolation of temporal hierarchical mobility networks during COVID-19," Phil. Trans. R. Soc. A **380**, 20210116 (2022).
[12]M. Newman, *Networks: An Introduction* (Oxford University Press, 2010).
[13]P. Hage and F. Harary, "Eccentricity and centrality in networks," Soc. Networks **17**, 57–63 (1995).
[14]L. Katz, "A new status index derived from sociometric analysis," Psychometrika **18**, 39–43 (1953).
[15]F. Morone and H. A. Makse, "Influence maximization in complex networks through optimal percolation," Nature **524**, 65–68 (2015).
[16]L. C. Freeman, "A set of measures of centrality based on betweenness," Sociometry **40**, 35–41 (1977).
[17]C. Fan, L. Zeng, Y. Sun, and Y.-Y. Liu, "Finding key players in complex networks through deep reinforcement learning," Nat. Mach. Intell. **2**, 317–324 (2020).
[18]P. Chen, M. Qi, X. Lu, X. Duan, and J. Kurths, "Efficient network immunization strategy based on generalized Herfindahl–Hirschman index," New J. Phys. **23**, 063064 (2021).
[19]P. Chen, M. Qi, L. Yan, and X. Duan, "Diffusion capacity analysis of complex network based on the cluster distribution," Chaos Soliton. Fract. **178**, 114329 (2024).
[20]R. Cohen, S. Havlin, and D. Ben-Avraham, "Efficient immunization strategies for computer networks and populations," Phys. Rev. Lett. **91**, 247901 (2003).
[21]Y. Bu, S. Gregory, and H. L. Mills, "Efficient local behavioral-change strategies to reduce the spread of epidemics in networks," Phys. Rev. E **88**, 042801 (2013).
[22]S. Chen and X. Lu, "An immunization strategy for hidden populations," Sci. Rep. **7**, 3268 (2017).
[23]Y. Liu, H. Sanhedrai, G. Dong, L. M. Shekhtman, F. Wang, S. V. Buldyrev, and S. Havlin, "Efficient network immunization under limited knowledge," Natl. Sci. Rev. **8**, nwaa229 (2021).
[24]M. Qi, S. Tan, P. Chen, X. Duan, and X. Lu, "Efficient network intervention with sampling information," Chaos Soliton. Fract. **166**, 112952 (2023).
[25]G. Lobinska, A. Pauzner, A. Traulsen, Y. Pilpel, and M. A. Nowak, "Evolution of resistance to COVID-19 vaccination with dynamic social distancing," Nat. Hum. Behav. **6**, 193–206 (2022).
[26]M. S. Granovetter, "The strength of weak ties," Am. J. Sociol. **78**, 1360–1380 (1973).
[27]R. M. Anderson and R. M. May, *Infectious Diseases of Humans: Dynamics and Control* (Oxford University Press, 1991).
[28]A.-L. Barabási and R. Albert, "Emergence of scaling in random networks," Science **286**, 509–512 (1999).
[29]J.-P. Onnela, J. Saramäki, J. Hyvönen, G. Szabó, D. Lazer, K. Kaski, J. Kertész, and A.-L. Barabási, "Structure and tie strengths in mobile communication networks," Proc. Natl. Acad. Sci. **104**, 7332–7336 (2007).
[30]R. Grassi, F. Calderoni, M. Bianchi, and A. Torriero, "Betweenness to assess leaders in criminal networks: New evidence using the dual projection approach," Soc. Networks **56**, 23–32 (2019).
[31]A. Lancichinetti, S. Fortunato, and F. Radicchi, "Benchmark graphs for testing community detection algorithms," Phys. Rev. E **78**, 046110 (2008).

[32]J. M. Kumpula, J.-P. Onnela, J. Saramäki, K. Kaski, and J. Kertész, "Emergence of communities in weighted networks," Phys. Rev. Lett. **99**, 228701 (2007).
[33]X. Lu, "Linked ego networks: Improving estimate reliability and validity with respondent-driven sampling," Soc. Networks **35**, 669–685 (2013).
[34]B. Karrer and M. E. J. Newman, "Stochastic blockmodels and community structure in networks," Phys. Rev. E **83**, 016107 (2011).
[35]A. Decelle, F. Krzakala, C. Moore, and L. Zdeborová, "Asymptotic analysis of the stochastic block model for modular networks and its algorithmic applications," Phys. Rev. E **84**, 066106 (2011).
[36]S. Maslov and K. Sneppen, "Specificity and stability in topology of protein networks," Science **296**, 910–913 (2002).
[37]V. D. Blondel, J.-L. Guillaume, R. Lambiotte, and E. Lefebvre, "Fast unfolding of communities in large networks," J Stat. Mech.: Theory Exp. **2008**, P10008 (2008).